The effects of pH and stress on seawater corrosion and conservation of copper and its alloys

Ian Donald MacLeod* and Anne-Sophie Romanet
Department of Materials Conservation
Western Australian Museum
Cliff Street
Fremantle, Western Australia 6160 Australia
Fax: + 61 8 93357224
Email: ian.macleod@museum.wa.gov.au

Abstract

The corrosion of copper, brass and bronze artefacts has been shown to be very sensitive to alloy composition and to stresses associated with both the manufacturing processes and those induced during the wrecking process. The impact of defects from gas porosity, and the changes in surface area as the pits are filled are emptied of corrosion products, has a direct bearing on the ultimate fate of the objects. From the way in which the corrosion rates change with pH it has been possible to determine the reasons behind occasional spectacular collapse of artefacts during storage.

Keywords

Copper, brass, bronze, shipwrecks, pH, corrosion, stress, defects

Introduction

Metallic artefacts recovered from historic shipwrecks exhibit a much greater variability in corrosion resistance than would be anticipated on the basis of their apparently similar elemental composition. Previous research has determined some of the reasons behind such differences (MacLeod and Pennec 1990: MacLeod 1994). By comparing freshly polished and heavily corroded surfaces of the same artefacts it is possible to see how corrosion changes the materials performance. Since "bronze disease" often occurs after many years of storage (Robbiola 1997: Paterakis 1998) it was important to study the way in which changes in pH affected corrosion rates. We needed to determine if there were any critical pH values that lead to collapse of the artefacts (Gilbert 1982: Pourbaix 1972). Similar studies have been made using the PEG 400/H_2O system, which relates to the treatment of composite wood and copper alloy artefacts (MacLeod and Romanet forthcoming).

Experiments

Bronze sheathing nails and a brass drift bolt from HMS *Sirius* (1790) had been in the sea for 200 years whilst the bronze and brass nails from the American China Trader *Rapid* (1811) were recovered after 168 years. Copper bolts from the French-built ex-slave-trader James *Matthews* (1841) had been buried for 130 years. The composition of the bolts and nails is listed in Table 1; the wear patterns indicate that they had been used in the construction of the vessels.

The corrosion experiments were performed using a VersaStat EGG Princeton Applied Research potentiostat, with the data recorded using the M352 Softcorr corrosion software. The potentiostat was controlled by a National Instruments PCMCIA-GPIB interface card. The scan rate was 1 mV/sec with scan range ± 250 mV around the open circuit potential (E_{oc}). Twin carbon-rods, in 3M potassium nitrate salt bridges, were the auxiliary electrodes. Preparation of the sectioned metal artefact electrodes has been previously described (MacLeod and Pennec 1990). The samples were exposed to sea water for periods of several weeks and then stored dry, without desalination, for seven years, which simulated poor storage conditions on aged artefacts.

Table 1. Composition of the copper alloys from historic shipwrecks.

Registration no.	Cu	Sn	Zn	Pb	Sb	Ni	Ag	Fe	As	Bi
Copper bolts										
JM 150/T 13	98.380	0.049	0.0037	0.101	0.027	0.021	0.108	0.002	0.340	0.077
JM 160/T8	98.630	0.074	0.0025	0.109	0.009	0.047	0.104	0.002	0.290	0.255
Brass fittings										
RP 0000/T 13	70.040	0.320	26.390	1.900	0.049	0.074	0.078	0.165	0.022	0.014
51 15	67.700	0.040	31.500	0.667	0.009	0.027	0.016	0.037	0.046	0.017
Bronze fittings										
RP 5004/T 11	90.300	7.460	0.024	0.810	0.545	0.086	0.151	0.086	0.042	0.231
51 228 B	90.000	8.000	0.768	0.468	0.005	0.018	0.053	0.513	<0.02	0.102

* Author to whom correspondence should be addressed

Table 2. Physical properties of the copper alloys.

Registration no.	Geometric area cm^2	Electrochemical area cm^2	Microhardness HV	Density g/cm^2	Equivalent mass g/mol
Copper bolts JM 150/T 13	1.47	7.3	86-146	8.92	63.01
JM 160/78	1.35	3.7	145-205	8.92	63.73
Brass fittings RP 0000/T 13	0.9	10.5	132-160	8.52	66.20
SI 15	2.1	31.4	80-149	8.46	65.08
Bronze nails RP 5004/T11	0.25	1.7	138-184	8.79	68.57
SI 228 B	0.22	2.9	82-143	8.80	68.10

The physical properties of the alloys are listed in Table 2 (MacLeod and Pennec 1990: MacLeod 1994). Prior to and during the corrosion experiments, the electrodes were photographed under a binocular microscope (x 120) and details of the patina were noted. Because of the experimental set up, the net anodic current in each scan was greater than the net cathodic current, which results in a gradual stripping of the aged surface. Each data set was repeated up to 20 times, especially if there was a marked departure from previously recorded data, in order to obtain reproducible results.

The data were analysed by the Softcorr program, using a curve-fitting routine to establish the values of the anodic (β) and cathodic (β) Tafel slopes of the oxidation and reduction reactions according to the Tafel relationship, shown in equation 1:

$$\eta = a - b \log I \quad (1)$$

The *a* term relates to the inherent rates of the electrochemical processes under reversible conditions, where $a = \beta \log i_0$ and i_0 is the exchange current density at the reversible potential E^0. The β value is the slope of the current-voltage curve, $(\delta\eta/\delta_{\log I})$ where η is the over potential and *i*, the corrosion current. The electrochemical corrosion rate can be converted from $\mu A.cm^{-2}$ to mm/year according to equation 2:

$$i_{\text{corrosion .mm/yr}} = 1.3 \times 10^{-4} \, i_{\text{corr}} \, (EW) \, d^{-1} \quad (2)$$

with EW the equivalent mass, based on the percentage of elements present in the alloy, and *d* is the density of the alloy in $g.cm^{-3}$ and i_{corr} is the corrosion rate in $\mu A.cm^{-2}$. The corrosion rates reported in this paper are based on the effective electrochemical area of the artefacts, which includes the effects of surface roughness and gas porosity. Periodically the software could not recognise the shape of the current voltage curve, due to multiple passivation peaks, and in these cases the default Stern-Geary values of 100 mV each for the anodic and cathodic Tafel slopes were used.

Electrolyte solutions

Seawater of 35.6‰ from Bathers Bay, Fremantle, was filtered through paper to remove debris and then stored in a refrigerator at 10°C until it was needed. Without the use of salt bridges to separate the auxiliary electrodes from the test solutions, the pH would vary by ±0.18 over six scans. The reference electrode was connected to the working solution through a Luggin capillary to minimise resistance effects. Surface examination helped establish which patina changes could be correlated with either passivation plateaus and the peak potentials (E_p) on the anodic scans or changes in the slope of the oxygen reduction curve.

Results and discussion

Copper artefacts

Both fittings had a primary patina of Cu_2O, with a patchy a secondary layer of $Cu_2(OH)_3Cl$. The micro-droplets of lead dispersed throughout the metal, along with inclusions of Cu_20 and Cu_2S,

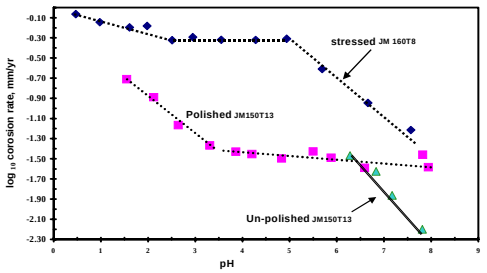

Figure 1. Effect of pH and polishing on the corrosion of copper fastenings from *James Matthews*

do not appear to exert a major influence on the corrosion phenomena. The effects of changing pH of the seawater on the two copper bolts JM 150/T13 and JM 160/T8 are summarised in Figure 1. Prior to repolishing, the bolt JM 150/T13 showed a high degree of sensitivity to pH with the log of the corrosion rate defined by equation 3 for the range 7.81 <pH>6.28,

$$^{\text{JM 150T13 before polishing}}\ log\ i_{\text{corrosion. mm/yr}} = 1.65 - 0.490\ \text{pH} \quad (3)$$

The behaviour of the stressed bolt JM 160/T8 over the range 7.57<pH>4.94 showed a similar logarithmic dependence, shown in equation 4:

$$^{\text{JM 160T8}}\ log\ i_{\text{corrosion. mm/yr}} = 1.366 - 0.344\ \text{pH} \quad (4)$$

By choosing a pH common to both domains, it is possible to use the equations to determine the relative differences in corrosion rates. At pH 7.0 the calculated corrosion rate for the stressed bolt is 0.091 mm/yr and 0.017 mm/year or roughly 5½ times lower for the less stressed metal. The corrosion rate of this bolt between 4.94<pH>2.51 was varied and the slope was approximately -0.03/pH but for the range 2.51 <pH>0.47 it conformed to another logarithmic relationship given by equation 5:

$$^{\text{JM 160T8}}\ log\ i_{\text{corrosion. mm/yr}} = -0.010 - 0.124\ \text{pH} \quad (5)$$

Since the less-stressed bolt was polished after the initial alkaline scans, a direct comparison of the behaviour of the two bolts over the entire range is not possible. The corrosion rate of the polished sample remained essentially independent of pH over the range 7.94<pH>3.86, but nevertheless it was higher than the corroded sample had been up to a pH of 6.28 (See Fig. 1). This change is due to the removal of the corroded metal-seawater interface, which leaves a much more uniform surface with a lowered electrochemical surface area. Once the solution became more acidic the corrosion rate began to increase significantly, with the data being described by equation 6, over the range 3.31 <pH>1.55:

$$^{\text{JM 150T13 after polishing}}\ log\ i_{\text{corrosion. mm/yr}} = -0.103 - 0.387\ \text{pH} \quad (6)$$

The similarity of the slope of equations 4 and 6 is probably due the same corrosion mechanism. The rapid increase in corrosion rate, which occurs at much less acidic solutions for the more highly stressed metal, was accompanied by a flow of the unstable yellow-brown fine precipitate CuOH from the sample. Ridges increased corrosion activity followed the lines of stress associated with distortion along the axis of the grains (MacLeod and Pitrun 1988). The rapid increase in corrosion rate stopped abruptly at pH 5 and remained independent of pH until a value of 2.3. Below this pH, the corrosion rate became very sensitive to pH whereas the less-stressed bolt only began to show an increased sensitivity of corrosion rate to pH below 2.9. The Pourbaix diagram of copper in seawater (Bianchi and Longhi 1973) shows that CuCl is more stable than Cu_2O below a pH of 5.3; the plateau regions correspond to the stability zone of CuCl. The formation of soluble copper(l) species such as $CuCl_2^-$ forms a vital part of the mechanism associated with the dissolution of copper in acidic chloride solutions (Fritz 1980; Braun and Noble 1979). The breakdown of the CuCl film on both samples occurs at a similar pH as free Cu^{2+} is formed; at this pH the metals are uniformly attacked. At pH 1.5, the more highly stressed nail was corroding three times faster than the less stressed sample.

The most important implication of this observation for conservators is that once the crevice pH falls below 2.5, there will be a massive increase in the rate of deterioration of the untreated shipwreck or archaeological artefact. Immersion into alkaline solutions and retention of some electrolyte in the interstices of the metal has real advantages in preventing rapid decay in storage. It also explains why objects that have been subjected to great stress corrode much more readily than those that have annealed structures. Since small amounts of antimony tend to inhibit intergranular corrosion, the higher levels of this impurity in the less-stressed bolt would also tend to make it less susceptible to chemical attack than the stressed bolt. The stressed bolt has

three times as much bismuth and since this element makes copper much less ductile, the worked structures are very prone to intergranular attack. The data also indicate that objects with aged surfaces are more resistant to the adverse effects of poor storage than are cleanly polished surfaces.

Brass artefacts

The structure of the aged bolt from HMS *Sirius (*SI 15) consisted of equiaxed grains with black intergranular corrosion boundaries. The alloy has a two-phase structure of both of and α an β (zinc-rich) at the grain boundaries, despite having 0.5% less zinc than the formal amount needed for a duplex brass. The patina was dominated by cuprite overlain by green corrosion products at the edges and in the middle of the section. After several scans the initial patina had become patchy which revealed gold coloured areas of parent metal and by pH 6.76 the surface was rough and yellow/brown. As the pH was lowered to 6.1, the profile at the intergranular boundaries is reduced to that of the plane of the electrode and the whole surface was rough. At pH 5.44 there are a few islands silver-grey "CuCl" at the edges. Over the range 7.97<pH>5.44, the log of the corrosion rate is given by equation 7:

$$^{\text{SI 15}}\, log\ i_{\text{corrosion. mm/yr}} = -0.671 - 0.323\ \text{pH} \qquad (7)$$

The brass nail shows essentially the same sensitivity of corrosion rate to changes in the pH as the stressed copper bolt from *James Matthews* but with different intercept values. At pH 7.0, the *James Matthews* copper bolt is corroding 3½ times as fast as the *Sirius* brass fitting.

The reason for the fall in corrosion rate between pH 5.4-5.2 is the formation of "CuCl" films. After "CuCl" species have covered much of the surface, the slope of the log plots fell to -0.091 for the range 4.79<pH>2.89. At the alkaline end of this range the intergranular boundaries were black-red; the black corrosion products probably containing hydrated zinchydroxysulphate, $ZnSO_4 3Zn(OH)_2.4\ H_2O$, and zinc oxide, ZnO (MacLeod 1991). These corrosion products tend to be formed from internal galvanic corrosion of the zinc-rich β phase. This phase "protects" the copper-rich α phase and this is why the brass still exhibited some sensitivity to pH, whereas the copper fittings were pH independent. The next jump in corrosion rate occurred as the patina of the intergranular boundaries changed to a brownish hue between 2.89<pH>2.29. After this pH, the slope of the corrosion rate was the "same" as for the previous range of pH at -0.094/pH change but the intercept was -0.843 compared with -0.428; this is equivalent to an increase in base corrosion rate by a factor of just more than 2½. The cause of the sudden jump in corrosion rate near pH 2.7 is probably due to the removal of protective corrosion products from the grain boundaries of the worked structure. The similarity of the slopes tip to pH as low as 0.53 indicates that it is the same corrosion mechanism controlling the oxidation and this is supported by the fact that the E_{corr} remained essentially constant over the range 5.5<pH>0.5. The overall patina was still mixed, with the three distinct areas as brown-yellow, grey and white giving rise to a series of passivation plateaus in the current voltage curves. When the curve-fitting program could "manage the passivation peaks" the average β values were 85±6 mV.

The *Rapid* brass nail was a single-phase alloy of 26.39% zinc with 0.32% tin, which provides a metallurgical zinc equivalent of 26.71 % zinc. The way in which the corrosion rate varied with pH was much the same as for the other alloys, with a series of pauses in the regular trend of increased decay with increased acidity. These "drops" are due to repassivation of the corroding surfaces as the surface concentration of ions is high enough to get an adherent precipitate to form. At pH 5.9, red Cu_2O forms at the edges of the dendrites and by pH 5.5 this had changed to a deep grey "CuCI" film with only a few bright red Cu_2O bright blue spots at the edges.

Despite some "bumps" of localised pitting activity for 2.56<pH>2.00, the 15 measurements from the single-phase *Rapid* brass had a correlation coefficient of 0.986 and the corrosion rate is given by equation 8. for 7.76<pH>0.40:

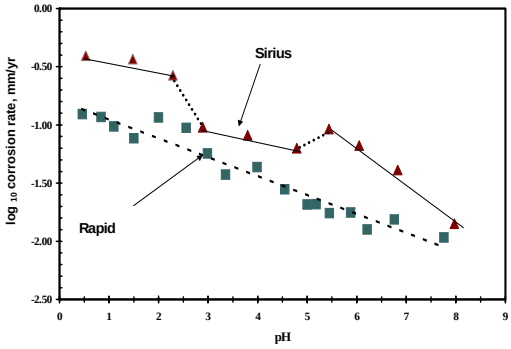

Figure 2. Effect of pH on the corrosion of brasses in seawater.

$$^{\text{Rapid 0000}}\log i_{\text{corrosion. mm/yr}} = -0.845 - 0.155\ \text{pH} \qquad (8)$$

The slope of the corrosion rate vs pH plot in equation 8 is similar to the value of-0.124 observed for the stressed copper in the most acidic solutions. Formation of passive films will affect the relative ease of oxidation, which accounts for the way in which the anodic Tafel slope (β_a) changes from 75 ± 2 mV (8<pH>5) to 86 mV between 3.4<pH>2.0 and then back to its previous value.

When comparing the two brasses, it is clear that the two-phase *Sirius* brass exhibits twice the sensitivity to pH changes over the range 8.0<pH>5.4, which is the zone in which Cu_2O is more thermodynamically stable than "CuCl (See Fig. 2). Once this region has been passed, the *Rapid* brass is more sensitive to pH by a factor of 1.65 times the *Sirius* brass. It should be noted that the *Rapid* brass has an as-cast structure whereas the *Sirius* has been worked and this mechanical deformation would increase the relative corrosion rates over and above the impact of the higher zinc content. Since both brasses show a logarithmic dependence of corrosion rate with pH, it is vital to avoid any storage environments that are acidic and to consider the routine use of alkaline desalination treatments.

Bronze artefacts

The wreck of HMS *Sirius* produced thousands of bronze sheathing tacks, of which SI 228-B was the subject of extensive analysis (MacLeod 1994). When the experiment began, the corroded 8% tin bronze (0.8% zinc) bronze had gas porosity pits filled with corrosion products. In the pH range 8<pH>5.4, the corrosion rate showed a logarithmic dependence on pH (equation 9), with the slope being similar to the *Rapid* brass nail (equation 8):

$$^{\text{Sirius 8<pH>5.4}}\log i_{\text{corrosion rate mm/yr}} = -0.37 - 0.19\ \text{pH} \qquad (9)$$

Over this pH range, the E_{corr} fell by 34 mV/pH, the anodic Tafel slope increased from 187 to 566 mV while the cathodic Tafel slope the β_a value decreased from 171 to 148 mV. A change in corrosion mechanism had clearly taken place during repeated scans. The way in which both the corrosion rate and the E_{corr} changed are consistent with increases in the anodic exchange current density as the copper rich phases are gradually exposed as the protective tin corrosion products are removed from the surface. Below a pH of 5.4, the β_a values returned to 227 ± 15 mV and the corrosion rate remained independent of pH until a value of 3.3 was reached. This pH independent range had been observed with *the James Matthews* stressed copper bolt and to a lesser extent, with the *Sirius* duplex brass bolt.

The corrosion rate showed an increased logarithmic dependence on pH, see equation 10, between pH 3.3 and 1.8:

$$^{\text{Sirius 3. 3 <pH>1.8}}\log i_{\text{corrosion rate mm/yr}} = -0.74 - 0.28\ \text{pH} \qquad (10)$$

The slope of equation 10 is similar to the Sirius brass bolt in the range 7.9<pH>5.4 where the slope was -0.323. As the pH fell, the β_a value continued to fall from 227 ± 15 mV to 135 ± 44 mV for 3.3<pH>1.8 which is indicative of copper phases controlling oxidation. At the same time the b_c decreased from 171 to 148 mV which is consistent with easier cathodic reduction of oxygen on the a phase. Catastrophic pitting of the samples occasionally takes place in acidic seawater solutions when the corrosion rate increases by more than five times above the average value for that pH. Such episodes are followed by rapid repassivation.

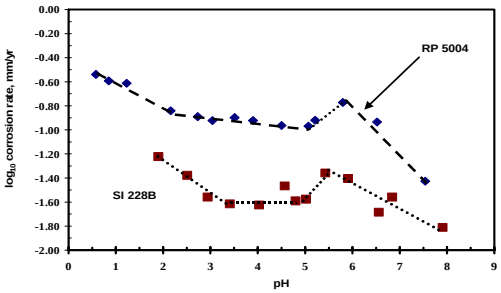

Figure 3. Effect of pH on the corrosion of bronzes in seawater.

The bronze nail *Rapid* 5004 shows a greater sensitivity to pH than the Sirius nail, despite having 0.5% less tin (See Fig. 3). It exhibits the same type of logarithmic dependence of corrosion rate and for the range 7.6<pH>5.8, the corrosion rate is given by equation 11:

$$^{\text{Rapid 7.6<pH>5.8}}\log i_{\text{corrosion rate mm/yr}} = +1.51 - 0.36\ \text{pH} \qquad (11)$$

At neutral pH 7.0, the calculated corrosion rates show that the *Rapid* bronze is corroding nearly five times as fast as the *Sirius* bronze. The dark brown patina showed

some white tin corrosion products at pH 6.5 and some Cu_2O/CuCl by pH 5.8. A 36% fall in the corrosion rate between pH 5.8 and pH 5 corresponded to the formation of some light yellow $Sn(OH)_3Cl$, a few cuprite spots in the centre and white products on the edge. This had been converted by pH 4.5 to a thick grey-white patina (SnO_2). Over the range 3.0<pH>0.3, the corrosion rate is given by equation 12:

$$^{\text{Rapid } 3.0<pH>0.3}\ log\ i_{\text{corrosion rate mm/yr}} = -0.29 - 0.16\ pH \qquad (12)$$

The diminished sensitivity to pH is due to a change in mechanism from being controlled by dissolution of a mixed tin/copper oxide patina in the more alkaline range to a copper patina in more acidic solutions. The β_a for pH $\geq$ 4 was 103 ± 4 mV while for more acidic solutions β_a fell to 78 ± 10 mV. The greater sensitivity of the Sirius bronze to pH, in acidic seawater, may be a reflection of the higher tin content and the 0.5% iron present in the alloy which also makes it more prone to internal galvanic corrosion attack. Since the Rapid bronze nail has a very porous structure and significant amounts of "tin sweat" at the as-cast edges, it is likely that the higher overall corrosion rate is due to the uneven distribution of tin across the surface.

References

Bianchi G and Longhi P. 1973. Copper in sea-water, potential-pH diagrams. *Corrosion Science* 13: 853-864.

Braun M and Noble K. 1979. Electrodissolution kinetics of copper in acidic chloride solutions. *J Electrochem Soc* 126: 1666-1671.

Chase WT. 1994. Chinese bronzes: casting, finishing, patination and corrosion. In: DA Scott, J Podany, BB Considine, eds. Ancient and historic metals conservation and scientific research. Los Angeles: Getty Conservation Institute: 265-278.

Fritz JJ. 1980. Chloride complexes of CuCl in aqueous solution. *Journal of physical chemistry* 84:2241-2246.

Gilbert PT. 1982. A review of recent work on corrosion behaviour of copper alloys in sea water. *Materials performance* 21: 47-53.

House Cl and Kelsall GH. 1984. Potential-pH diagrams for Sn/H_2O-Cl system. *Electrochimica Acta* 29(10): 1459-1464.

MacLeod ID. 1991. Identification of corrosion products on non-ferrous metal artefacts recovered front shipwrecks. *Studies in conservation* 36(4): 222-234.

MacLeod ID. 1994. Conservation of corroded metals -a study of ships' fastenings from the wreck of HMS Sirius. In: DA Scott, J Podany, BB Considine, eds. Ancient and historic metals conservation and scientific research. Los Angeles: Getty Conservation Institute: 265-278.

MacLeod ID and Pennec S. 1990. The effects of composition and microstructure on the corrosivity of copper alloys in chloride media. In: ICOM Committee for Conservation, 1990 Preprints 9th Triennial Meeting, Dresden. Vol. II: 732-739.

MacLeod ID and Pitrun M. 1988. Metallography of copper and its alloys recovered from nineteenth century shipwrecks. In: JR Prescott, ed. Archaeometry: Australasian studies. Adelaide: University of Adelaide: 121-130.

MacLeod ID and Romanet A-S. Forthcoming. Effects of pH and PEG 400 concentration on the corrosion and conservation of composite wood and copper alloy artefacts recovered from historic shipwrecks. Bulletin of the Australian Institute for Maritime Archaeology.

Paterakis AJ. 1998. Archaeological metals in the ancient Athenian Agora. In: W Mourey and L Robbiola, eds. Metal 98: Proceedings of the International Conference on Metals Conservation, Draguignan, France, May 1998. London: James & James: 253-259.

Pourbaix M. 1972. Significance of protection potential in pitting, inter-granular corrosion and stress-corrosion cracking. Journal of less common metals 28: 51-65.

Robbiola L. 1997. Standard nature of the passive layers of buried archaeological bronze. The example of two Ronian half-length portraits. *In: Metal 95- Proceedings of the International Conference on Metals Conservation,* Sernur-en-Auxois, France, September 1995. London: James & James: 109-117.

Tanabe Z. 1972. Protective films on copper alloys in 3% sodium chloride aqueous solution. Sumito *Light Metal Technical Reports* 13(4): 168-177.